

**A TRUE OFF-SET SELF-ALIGNED PROCESS FOR HIGH  
EFFICIENCY Ku-BAND POWER FETS <sup>(1)</sup>**

Kouichi Wakamoto, Kimihiko Imura, Masahiko Yamamoto, Satoshi Shimoyama, Takehiko Kameyama, Masao Isomae, Yukio Okubo, Mikiharu Ohoka, Takashi Nagashima, Nippon Mining Co., 3-17-35 Niizo-Minami, Toda, Saitama, Japan 335. Tel: 0484-45-6607.

Domingo A. Figueiredo (\*), Lyle H. McCarty(\*), Chung-Yi Su, Michael Yam, Sanehiko Kakihana, Menlo Industries Inc., 44060 Old Warm Springs Boulevard, Fremont, California, USA 94538. Tel: 415-659-9755.

(1) United States Patent No. 4792531: December 20, 1988.

(\*). These authors are presently at Nippon Mining Co., 3-17-35 Niizo Minami, Toda, Saitama, Japan 335.

**ABSTRACT**

A new off-set self-aligned process has been used to fabricate a  $2 \times 3000 \mu\text{m}$  gate width internally matched power FET which at 14 GHz has produced 34.4 dBm output power, 6 dB gain and 32 % added efficiency at the -1 dB gain compression point with a power combining efficiency of  $\approx 96 \%$ . The high combining efficiency is attributed to the close parameter match of the self-aligned power FETs.

**INTRODUCTION**

Today's commercially available power FETs operating at Ku-band employ a combination of epitaxially grown or ion implanted active layers which require single or multiple recess structures ranging in depth from 1600 Å to 4000 Å (1-8). These structures demand strict controls on the active layer fabrication, lithography and gate recess formation in order to obtain repeatable DC and RF parameters. Several self-aligned processes have been recently developed for digital and low noise applications (9,10,11). Because the ohmic (or  $n^+$ ) contact regions are adjacent to the gate, high drain bias - such as required for power operation - is not possible. A process with source-gate self-alignment and advanced substrate technology has recently demonstrated excellent large signal performance (12).

This work describes and demonstrates a process whereby the source, gate, and drain openings are defined simultaneously. The source-gate self-alignment permits a relatively shallow gate recess (0-600 Å) which preserves the uniformity of the active layer. The self-aligned gate-drain spacing results in a large and uniform gate-drain breakdown voltage which is specially important for power applications.

**PROCESS DESCRIPTION**

The principal fabrication steps of the new process are depicted in Figure 1.

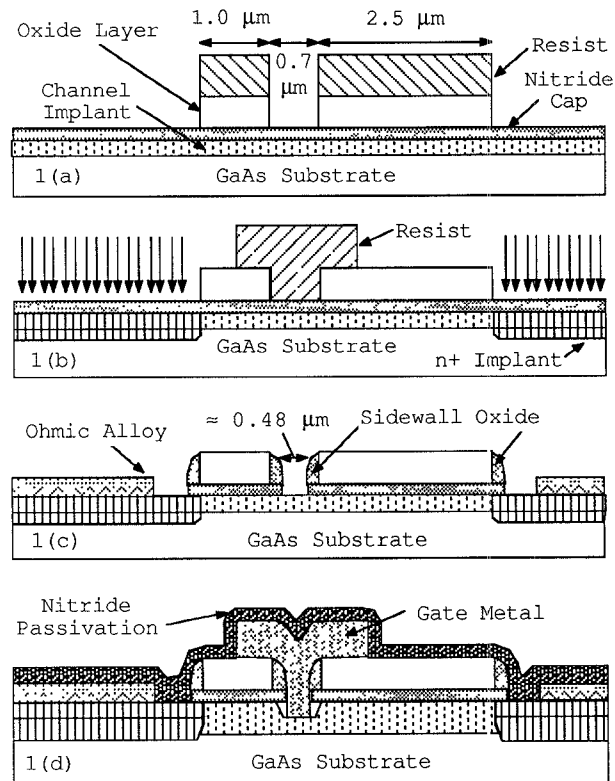


Figure 1: Cross sectional view of the self-aligned process: 1(a): after channel implant, nitride cap, anneal, first oxide deposition and self-aligned patterning steps. 1(b): after  $n^+$  implant. 1(c): after second oxide deposition (sidewall), oxide and nitride etch, and ohmic alloy. 1(d): after gate definition, and final passivation.

After a selective Si implant, a  $\text{Si}_3\text{N}_4$  cap is deposited to prevent GaAs decomposition during furnace annealing. The peak carrier concentration is  $\approx 2 \times 10^{17}$  Si atoms/cm<sup>3</sup>. The channel thickness is  $\approx 2500 \text{ \AA}$  thick. An  $\text{SiO}_2$  layer is sputter deposited and patterned with the self-aligned source, gate and drain openings. The digitized source to gate and gate to drain spacings are 1 and 2.5  $\mu\text{m}$  respectively. The gate opening is 0.7  $\mu\text{m}$ . Refer to Figure 1(a). The  $\text{SiO}_2$  is selectively removed from the openings using  $\text{CHF}_3$  RIE. The gate area is masked with photoresist to protect it from the high energy, high dose  $n^+$  implant of the source and the drain contact regions as in Figure 1(b). After the  $n^+$  region is annealed, a second layer of  $\text{SiO}_2$  is deposited on the self-aligned source, gate and drain pattern. RIE is again employed to remove the second  $\text{SiO}_2$  layer and the nitride cap. Because the vertical reactive ion etch rate is greater than the lateral etch rate, the gate opening can be controlled by increasing or decreasing the thickness of the second oxide. Thus, sub-half-micron gate openings are made possible without having to resort to sub-half-micron lithography. A cross sectional view of the sidewall oxide is shown by Figure 1(c). The uniformity of the gate length across a wafer is depicted by Figure 2; the second  $\text{SiO}_2$  thickness is  $\approx 3000 \text{ \AA}$  in this case.

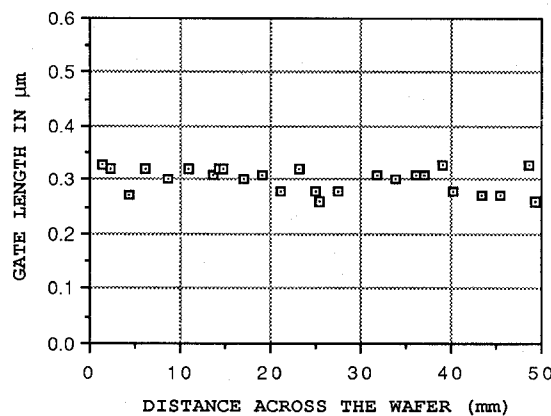


Figure 2: Typical gate length variation across a 50 mm diameter wafer.

After ohmic contacts are formed using standard alloy techniques, the gate opening is patterned and a shallow gate recess ( $\leq 600 \text{ \AA}$ ) is defined in the channel area. The recess depth, and the size of the gate metallization are controlled to optimize  $R_{ds}$ ,  $C_{gd}$  and alignment requirements. Ti-Pt-Au is used as the gate metallization. A  $\text{Si}_3\text{N}_4$  layer is deposited using plasma enhanced CVD as a final passivation dielectric, as shown in Figure 1(d). The

sources are interconnected using an airbridge plating process. After thinning the wafer to  $\approx 30 \mu\text{m}$  to reduce the thermal resistance, via holes are patterned and etched through to the source contacts. The

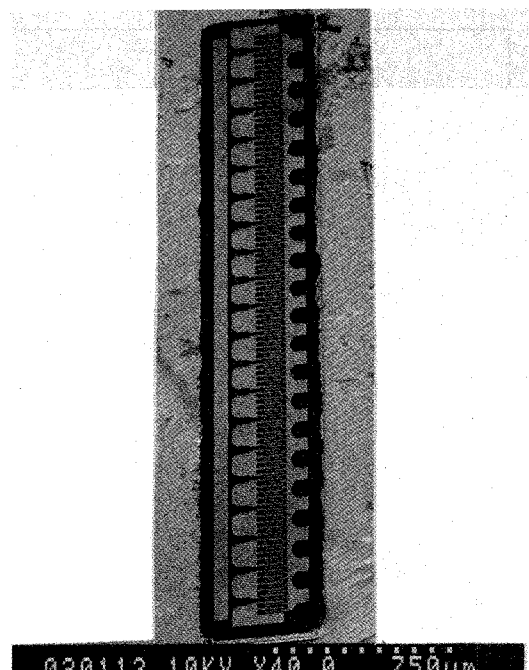


Figure 3: 16 mm gate periphery self-aligned power MESFET. The chip size is  $\approx 500 \mu\text{m} \times 3400 \mu\text{m}$ .

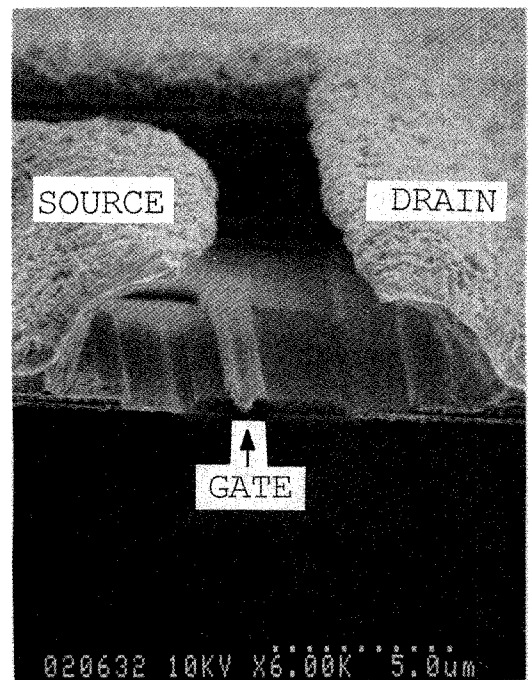


Figure 4: Cross section of finished chip showing the self-aligned structure (center).

backside is plated with Au and the wafer is then separated into chips using a dry chemical process. This technique reduces damage to the chips produced by standard scribe and separation techniques.

FETs with up to 16 millimeter gate widths have been fabricated using this process (see Figure 3.) The cross section of a finished device is shown by Figure 4. The second oxide layer deposition has been adjusted to give a final gate length  $\approx 0.48 \mu\text{m}$ .

### MICROWAVE RESULTS

Figure 5 shows the small signal model for a typical 750  $\mu\text{m}$  monitor FET under power bias measured from 1 to 18 GHz using microwave probes.

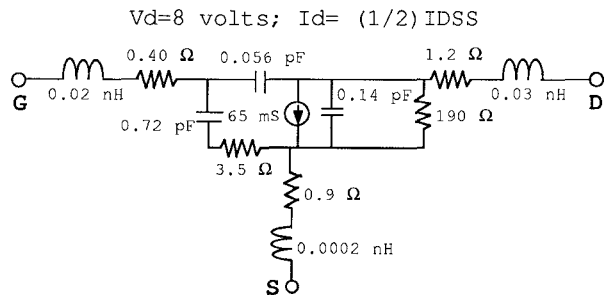


Figure 5: Small signal model for 750  $\mu\text{m}$  monitor FET; from microwave probe measurement from 1 to 18 GHz.

An internally matched power FET fabricated using two 3000  $\mu\text{m}$  gate width FETs has been tested at 14 GHz. The bias point was 50 % IDSS (800 mA) and Vd = 8 volts. The power and efficiency curves for this device are depicted by Figure 6: at the -1 dB gain compression point, the device produces 34.4 dBm power and 6 dB gain with  $\eta_{\text{add}} \approx 32 \%$ . Psat is  $\approx 34.8 \text{ dBm}$  or 503 mW/mm.

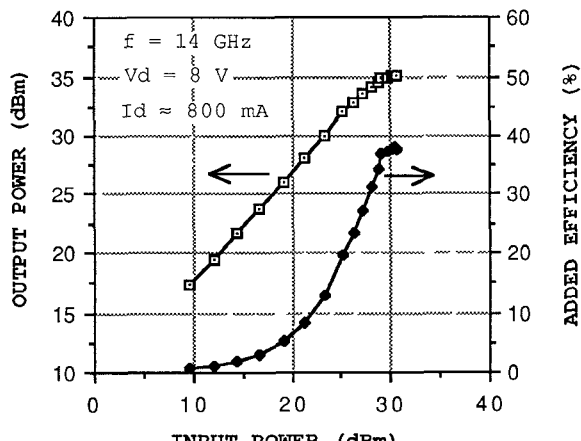


Figure 6: 2 x 3000  $\mu\text{m}$  internally matched FET power and efficiency performance at 14 GHz. Linear gain is  $\approx 7 \text{ dB}$ .

Figure 7 shows a similarly biased 750  $\mu\text{m}$  monitor FET. In this case, Psat  $\approx 25.92 \text{ dBm}$ , or  $\approx 521 \text{ mW/mm}$ . These results suggest that the power combining efficiency is better than 96 % for the IMFET. This achievement is attributed to the close parameter match resulting from using the new self-aligned process.

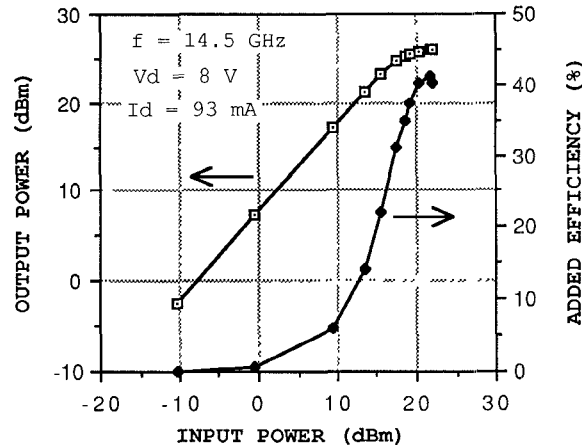


Figure 7: 750  $\mu\text{m}$  monitor FET power and efficiency performance at 14.5 GHz. Linear gain is  $\approx 7.8 \text{ dB}$ .

The 750  $\mu\text{m}$  monitor FET has also been evaluated at other frequencies and bias conditions. The results are summarized in TABLE(I).

| FREQ. (GHz) | P-1 dB (dBm) | G-1 dB (dB) | EFFICIENCY (%) | Vd (V) | Id      |
|-------------|--------------|-------------|----------------|--------|---------|
| 8           | 25.7         | 10.5        | 35             | 8      | 0.5IDSS |
| 9.5         | 25.1         | 9           | 32             | 8      | 0.5IDSS |
| 9.5         | 25.3         | 6.1         | 40             | 8      | 0.2IDSS |
| 14.5        | 25.3         | 6.8         | 35             | 8      | 0.5IDSS |
| 18          | 24.6         | 5.4         | 25             | 8      | 0.5IDSS |
| 18          | 25.1         | 3           | 31             | 8      | 0.2IDSS |

TABLE (I): 750  $\mu\text{m}$  Monitor FET with IDSS  $\approx 200 \text{ mA}$ .

### RELIABILITY

The drain to source burn-out voltage characteristics of a typical power FET were measured at room temperature using a Tektronix 370 programmable curve tracer. The pulse width was 80  $\mu\text{s}$  and the duty cycle was 100 Hz. Catastrophic failures occurred at Vd  $\approx 15, 27$  and 30 volts for 100% IDSS, 50% IDSS and pinch-off (defined at Vd = 2 volts and 1.5% IDSS) respectively.

After 3000 hours of High Temperature Storage (HTS) at 295  $^{\circ}\text{C}$  in air, the average drift of the critical parameters for a

sample of five FETs was as follows:  $\Delta IDSS \approx -15\%$ ,  $\Delta Gm \approx -8\%$  and  $\Delta Vpo \approx -9\%$ .

These results are attributed to the triple passivation of the active area. First, the channel is covered with a layer of nitride which is used as the capping material during the channel anneal. Second, a layer of oxide is deposited on the cap and used to pattern the self-aligned source gate and drain openings, and finally, a film of silicon nitride is deposited by plasma enhanced Chemical Vapor Deposition to assure hermeticity.

### CONCLUSIONS

A new off-set self-aligned process for the fabrication of power FETs has been demonstrated (efforts are now under way to improve the active layer for 18 GHz operation, test discrete devices with 16 mm gate widths, and implement power MMICs.) The new process has been used, but is not limited to, the production of analog microwave devices.

### ACKNOWLEDGEMENTS

The authors wish to gratefully acknowledge the following persons: Ms. Fumiko Yamasaki for lithography and related processing, Mr. Noriyuki Oyama for assembly of chips, Mr. Kiyotaka Kikuchi and Mr. Kazuo Shinohara for reliability testing, and Mr. Masaharu Murata, Mr. Masahiro Tsuchiya, and Mr. Harutoshi Saigusa for assistance with microwave characterization.

Finally, this work would not have been possible without the encouragement and faithful management support provided by Mr. Hiroshi Yasui, Dr. Takuzou Ogawa and Mr. Tatsuya Kamei.

### REFERENCES

- (1) H.M. Macksey, "Optimization of  $n^+$  Ledge Channel Structure for GaAs Power FET's", *IEEE Trans. Electron Devices*, vol. ED-33, No. 11, pp. 1818-1824, November 1986.
- (2) H.M. Macksey et. al, "Optimization of GaAs Power MESFET Device and Material Parameters for 15 GHz Operation", *IEEE Trans. Electron Devices*, vol. ED-27, No. 2, pp. 467-471, February 1980.
- (3) T. Noguchi and Y. Aono, "K- and Ka-Band Power GaAs FETs", *IEEE MTT-S Digest*, pp. 156-158, 1982.
- (4) Toshio Shino et. al, "High-Power GaAs FET's Prepared by Ion Implantation", *IEEE Trans. Electron Devices*, vol. ED-32, No. 11, pp. 2301-2306, November 1985.

(5) Y. Yamada et. al, "X AND Ku BAND HIGH POWER GaAs FETs," *IEEE MTT-S Digest*, pp. 847-850, May 1988.

(6) Madhu Avasarala and Ding-Yuan S. Day, "2.5-WATT AND 5-WATT INTERNALLY MATCHED GaAs FETs FOR 10.7-11.7 AND 14-14.5 GHz BANDS," *IEEE MTT-S Digest*, pp. 455-458, June 1986.

(7) Y. Kadowaki et. al, "A 6 WATT POWER GaAs FET FOR 14.0-14.5 GHz BAND," *IEEE MTT-S Digest*, pp. 845-847, June 1987.

(8) D. Bechtle et. al, "K-AND Ka-BAND HIGH EFFICIENCY AMPLIFIER MODULES USING GaAs POWER FETs," *MTT-S Digest*, pp. 849-852, June 1987.

(9) C. F. Wan et. al, "A COMPARISON STUDY OF GaAs E/D- MESFETs FABRICATED WITH SELF-ALIGNED AND NON-SELF-ALIGNED PROCESSES," *GaAs IC Symp. Tech. Digest*, pp 113-136, October 1987.

(10) T. Tambo et. al, "Low-Noise GaAs MESFET by Dummy-Gate Self-Alignment Technology for MMIC," *GaAs IC Symp. Tech. Digest*, pp. 49-52, October 1987.

(11) Kazuhiko ITO et. al, "A SELF-ALIGNED PLANAR GaAs MESFET TECHNOLOGY FOR MMICs," *GaAs IC Symp. Tech. Digest*, pp. 45-48, October 1987.

(12) A.E. Geissberger et. al, "HIGH-EFFICIENCY X- AND Ku-BAND GaAs POWER FET's FABRICATED USING REFRactory SAG TECHNOLOGY," *GaAs IC Symp. Tech. Digest*, pp. 309-312, November 1988.